

Supplement of Atmos. Chem. Phys., 18, 6511–6533, 2018  
<https://doi.org/10.5194/acp-18-6511-2018-supplement>  
© Author(s) 2018. This work is distributed under  
the Creative Commons Attribution 4.0 License.



*Supplement of*

## **Phenomenology of summer ozone episodes over the Madrid Metropolitan Area, central Spain**

**Xavier Querol et al.**

*Correspondence to:* Xavier Querol ([xavier.querol@idaea.csic.es](mailto:xavier.querol@idaea.csic.es))

The copyright of individual parts of the supplement might differ from the CC BY 4.0 License.

## SUPPLEMENTARY MATERIAL

### PTRMS measurements and O<sub>3</sub> Formation Potential (OFP)

A PTR-TOF-MS8000 (Ionicon Analytik Ges.m.b.H., Innsbruck, Austria) operating in H<sub>3</sub>O<sup>+</sup> mode was deployed at the ISCIII site from 04 to 19/07/2016. Detailed description of the instrument can be found in Graus et al (2010). The reaction conditions were a drift voltage of 545 V, a chamber temperature of 60°C and a drift pressure of 2.2 mbar resulting in an E/N of about 120 td. The time resolution was 1 min. The mass resolution, as well as the mass accuracy and the relative transmission efficiency were routinely verified using a 12 compounds gas standard including aldehydes, ketones and aromatics from m/z 45 to m/z 181 (100 ppb each in Nitrogen). The data was treated using the Software 2.4.2 software (Ionicon Analytik Ges.m.b.H., Innsbruck, Austria). The mixing ratios in pbb<sub>v</sub> are calculated using the ratio between the signal of the individual ions C<sup>+</sup> and the signal of the reagent ion H<sub>3</sub>O<sup>+</sup> taking into account the drift voltage (Udrift), drift temperature (Tact), drift pressure (pact) as well as the reaction rate of the ion with the H<sub>3</sub>O<sup>+</sup> ion (k) and the transmission of the compound (TR<sub>C+</sub>) relative to the transmission of the reagent ion (TR<sub>H<sub>3</sub>O+</sub>). K value from Cappellin et al. (2012) were used for the concentration calculation, when available. Otherwise, the default value (2.00x10<sup>-9</sup> cm<sup>3</sup>/s) was used. They are reported in table S1. Regarding formaldehyde, the water content correction procedure developed by Vlasenko et al (2010) was applied.

Ozone formation potential (OFP) were assessed on a basis of 24 VOCs or group of VOCs quantified (table S1), for which an unambiguous molecular identification can be inferred and a MIR (Maximum Incremental Reactivity) is available in the literature. The MIR scale is the incremental reactivity (IR) of a VOC computed for conditions in which the compound has its maximum absolute IR value (Carter, 1994). This generally occurs at a low VOC-to-NO<sub>x</sub> ratio in which the chemistry is VOC-limited. OFP corresponds thus to a maximum O<sub>3</sub> concentration formation for a VOC, or mix of VOCs (Carter, 1994). In this study, we used the updated MIR values from Carter (2009)(Table S1). For monoterpenes, a weighted MIR value has been calculated assuming a constant composition of 45% α-pinene, 18% β-pinene, 28% limonene, 7% myrcene and 2% camphene. These proportions were assessed from 2 Tenax cartridges analysis collected on 19/07/2016 at the ISCIII site. Total OFP (μg m<sup>-3</sup>) as well as the relative contribution of the 24 VOCs or group of VOCs are reported in table S1 for 3 selected days: 06/07/2016 (accumulation day), 14/07/2016 (transition day) and 13/07/2016 (venting day). For each day, we considered 3 distinct periods: Morning traffic peak (06:00-09:00 UTC), maximum insolation/biogenic VOC emissions period (11:00- 13:00 UTC), and evening traffic peak (19:30-21:30 UTC). Average daytime OFP (06:00-21:30 UTC) for each selected days as well as overall campaign average are also reported in table S1 and figure S1.

It's important to consider that the OFP reported here represent only partial assessment of the overall OFP in the MMA. This analysis does not consider any alkanes nor alkenes which may be very significant OFP contributors in urban environments (Duan et al., 2008, for example). The PTR-ToF-MS can only measure compounds with proton affinity higher than that of water (about 697 kJ mol<sup>-1</sup>) (Lindinger et al., 1998a, b), therefore compounds like methane (544 kJ mol<sup>-1</sup>), ethane (596 kJ mol<sup>-1</sup>), propane (626 kJ mol<sup>-1</sup>), butane (678 kJ mol<sup>-1</sup>), ethene (641 kJ mol<sup>-1</sup>) and acetylene (641 kJ mol<sup>-1</sup>) could not be detected. For higher molecular weight alkanes or

alkenes the fragmentation patterns are not specific enough to allow a proper identification and quantification.

Due to higher VOC concentrations, OFP are significantly higher during the accumulation period (06/07/2016) than during the transition (14/07/2016) and venting (13/07/2016) days. However, the relative contributions of the different VOC families stay relatively constant whatever period is considered (Figure S1). The total OFP is largely dominated by the impact of carbonyls representing between 42 and 67% of the total OFP, and particularly by formaldehyde and acetaldehyde. Aromatics and oxygenated aromatics show more variability with higher contributions during the morning traffic peaks (up to 27% of the total OFC during accumulation periods). However, the impact of the morning traffic emissions is compensated, all along the day, by the emissions of biogenic VOCs (isoprene and monoterpenes) and the formation of their main oxidation products (methylglyoxal, methacrolein, methyl vinyl ketone) (Table S1), contributing up to 16% of the OFP. Accumulation periods favouring the formation of O<sub>3</sub> from VOCs emitted and formed within the MMA, this result highlights the potential importance of biogenic emissions towards the O<sub>3</sub> concentrations observed in a large urban area such as Madrid, whose relative contribution to the OFP will increase with the distance to urban areas. However, as carbonyls and alkanes/alkenes are largely emitted by anthropogenic sources (vehicular emissions, mostly) and/or significantly produced by the oxidation of anthropogenic VOCs (for carbonyls), the anthropogenic emissions may still largely dominate the OFP. And because, it was not possible to include the, mostly anthropogenic, alkanes/alkenes in the OFP calculations the anthropogenic VOCs contribution to OFP should be considered as the minimum one.

## References

- Cappellin, L. et al., 2012. On Quantitative Determination of Volatile Organic Compound Concentrations Using Proton Transfer Reaction Time-of-Flight Mass Spectrometry, *Environmental Science & Technology*, 46, 2283-2290.
- Carter, W. P. L., 1994. Development of Ozone Reactivity Scales for Volatile Organic Compounds, *J. Air & Waste Manage. Assoc.*, 44, 881-899.
- Carter, W. P. L., 2009. Updated Maximum incremental reactivity scale and hydrocarbon bin reactivities for regulatory applications. Available at <https://www.arb.ca.gov/research/reactivity/mir09.pdf> (last access: 1 October 2017).
- Duan, J., Tan J., Yang L., Wu S., Hao J., 2008. Concentration, sources and ozone formation potential of volatile organic compounds (VOCs) during ozone episode in Beijing, *Atmospheric Research*, 88, 1, 25-35.
- Graus, M., Muller, M., Hansel, A., 2010. High Resolution PTR-TOF: Quantification and Formula Confirmation of VOC in Real Time, *Journal of the American Society For Mass Spectrometry*, 21, 1037-1044.
- Lindinger, W., Hansel, A., Jordan, A., 1998a. On-line monitoring of volatile organic compounds at pptv levels by means of proton-transfer-reaction mass spectrometry (PTR-MS) - Medical applications, food control and environmental research, *International Journal of Mass Spectrometry*, 173, 191-241.
- Lindinger, W., Hansel, A., Jordan, A., 1998b. Proton-transfer-reaction mass spectrometry (PTR-MS): on-line monitoring of volatile organic compounds at pptv levels, *Chemical Society Reviews*, 27, 347-354.
- Vlasenko, A., Macdonald, A. M., Sjostedt, S. J., Abbatt, J. P. D., 2010. Formaldehyde measurements by Proton transfer reaction – Mass Spectrometry (PTR-MS): correction for humidity effects, *Atmos. Meas. Tech.*, 3, 1055-1062.

Table S1. Ozone Formation Potential (OFP) and relative contribution of VOCs as measured by the PTR-ToF-MS (ISCI site) to the total OFP. <sup>1</sup>MIR (Maximum Incremental Reactivity,  $\mu\text{gO}_3$  per  $\mu\text{gVOC}$ ) are from Carter (2009), <sup>2</sup> [VOC] $\times$ MIR,  $\mu\text{g m}^{-3}$ . PTR-MS does not allow measuring alkenes and alkanes (mostly anthropogenic) and accordingly these were not included in the OFP calculations.

		06/07/2016				14/07/2016				13/07/2016				Avg Camp		
time UTC		6-9h	11-13h	19h30-21h30	6-21h30	6-9h	11-13h	19h30-21h30	6-21h30	6-9h	11-13h	19h30-21h30	6-21h30			
OFP tot ( $\mu\text{m}^{-3}$ ) <sup>2</sup>		299.3	193.9	211.4	199.1	87.6	85.3	83.8	96.6	77.9	92.0	80.8	94.0	155.4		
m/z	k [ $10^{-9}\text{cm}^3/\text{s}$ ]	Most probable compounds	MIR <sup>1</sup>	Relative contribution												
31.0178	2.00	Formaldehyde	9.24	20.5%	36.5%	32.5%	33.7%	39.5%	49.5%	43.3%	42.8%	45.6%	49.4%	47.1%	47.1%	35.5%
33.0335	2.14	Methanol	1.45	16.3%	12.8%	10.1%	12.7%	9.1%	9.1%	11.3%	8.9%	9.9%	10.0%	11.1%	9.7%	11.8%
45.0335	3.02	Acetaldehyde	6.34	12.1%	14.3%	16.0%	13.8%	12.6%	12.4%	9.5%	9.7%	12.1%	10.0%	9.9%	10.2%	14.7%
47.0128	1.99	Formic acid	0.062	0.1%	0.2%	0.1%	0.1%	0.1%	0.0%	0.0%	0.1%	0.1%	0.1%	0.1%	0.1%	0.1%
47.0491	2.18	Ethanol	1.25	0.5%	0.1%	0.5%	0.3%	0.7%	0.1%	0.6%	0.3%	0.8%	0.4%	1.0%	0.6%	0.6%
57.0335	3.05	Acrolein	7.24	1.6%	1.6%	1.5%	1.5%	1.8%	0.9%	0.6%	1.0%	1.6%	1.3%	1.5%	1.3%	1.4%
59.0491	3.32	Acétone	0.35	2.5%	3.1%	2.6%	2.9%	2.2%	2.5%	2.6%	2.4%	2.6%	2.8%	2.6%	2.7%	2.8%
61.0284	2.25	Acetic acid	0.66	2.2%	3.0%	2.6%	2.7%	2.0%	1.0%	0.8%	1.3%	2.2%	1.7%	1.1%	1.7%	2.4%
69.0699	1.96	Isoprene	10.28	4.1%	4.7%	4.2%	4.6%	3.9%	4.2%	7.2%	5.2%	4.5%	4.2%	6.2%	5.2%	4.7%
71.0491	3.05	Methacrolein/MVK	5.84	2.0%	3.4%	3.3%	2.8%	2.3%	4.5%	5.0%	4.0%	3.1%	2.7%	5.6%	3.7%	3.9%
73.0284	2.00	Methylglyoxal	16.02	3.9%	7.5%	5.2%	6.0%	0.5%	2.9%	0.7%	1.9%	2.4%	4.1%	2.8%	3.9%	5.1%
73.0648	3.28	Butanone	2	4.3%	1.6%	2.2%	2.3%	1.5%	1.1%	2.9%	1.6%	1.3%	1.4%	1.1%	1.4%	1.9%
75.0441	2.41	Methylacetate	0.067	0.0%	0.1%	0.1%	0.1%	0.0%	0.0%	0.0%	0.0%	0.0%	0.0%	0.0%	0.0%	0.1%
79.0542	1.93	Benzene	0.69	0.1%	0.1%	0.1%	0.1%	0.2%	0.1%	0.1%	0.1%	0.1%	0.1%	0.1%	0.1%	0.1%
87.0441	1.70	2,3 butanedione	2.61	0.8%	1.2%	1.0%	1.0%	0.4%	0.2%	0.1%	0.3%	0.5%	0.5%	0.3%	0.5%	0.8%
93.0699	2.08	toluene	3.88	9.2%	3.3%	7.5%	5.1%	2.9%	3.5%	6.9%	3.5%	3.1%	2.2%	2.5%	2.4%	4.8%
95.0491	2.18	phenol	2.69	0.1%	0.2%	0.2%	0.2%	0.1%	0.0%	0.0%	0.0%	0.1%	0.1%	0.1%	0.1%	0.1%
105.07	2.27	styrene	1.65	0.1%	0.1%	0.1%	0.1%	0.1%	0.0%	0.1%	0.1%	0.1%	0.0%	0.1%	0.1%	0.1%
107.049	3.82	benzaldehyde	-0.67	-0.1%	-0.1%	-0.1%	-0.1%	-0.1%	-0.1%	0.0%	-0.1%	-0.1%	-0.1%	-0.1%	-0.1%	-0.1%
107.086	2.26	C8 aromatics	7.48	14.2%	4.0%	6.8%	6.7%	11.7%	4.6%	4.7%	10.1%	6.2%	5.3%	3.4%	5.4%	5.6%
121.065	2.26	tolualdehyde	-0.59	-0.1%	0.0%	-0.1%	-0.1%	-0.1%	0.0%	0.0%	-0.1%	-0.1%	-0.1%	0.0%	-0.1%	-0.1%
121.101	2.41	C9 aromatics	5.65	2.9%	1.3%	2.3%	1.8%	6.4%	1.5%	1.6%	5.0%	1.4%	2.5%	1.4%	2.1%	1.9%
135.117	2.45	C10 aromatics	5.53	0.9%	0.4%	0.7%	0.6%	1.1%	0.4%	0.6%	0.7%	0.6%	0.4%	0.6%	0.5%	0.6%
137.132	2.43	monoterpenes	4.17	1.7%	0.8%	0.7%	1.0%	1.4%	1.1%	1.5%	1.2%	1.7%	0.9%	1.6%	1.4%	1.2%
		<i>By family</i>														
		Aromatics and O-Aromatics		27%	9%	18%	14%	22%	10%	14%	19%	11%	10%	8%	10%	13%
		Primary BVOCs		6%	5%	5%	6%	5%	5%	9%	6%	6%	5%	8%	7%	6%
		Secondary BVOCs		6%	11%	8%	9%	3%	7%	6%	6%	6%	7%	8%	8%	9%
		<i>Total BVOC</i>		12%	16%	13%	14%	8%	13%	14%	12%	12%	12%	16%	14%	15%
		Carbonyls (others)		42%	58%	56%	55%	58%	67%	59%	58%	64%	65%	63%	63%	57%
		Alcohol		17%	13%	11%	13%	10%	9%	12%	9%	11%	10%	12%	10%	12%
		Acids		2%	3%	3%	3%	2%	1%	1%	1%	2%	2%	1%	2%	2%

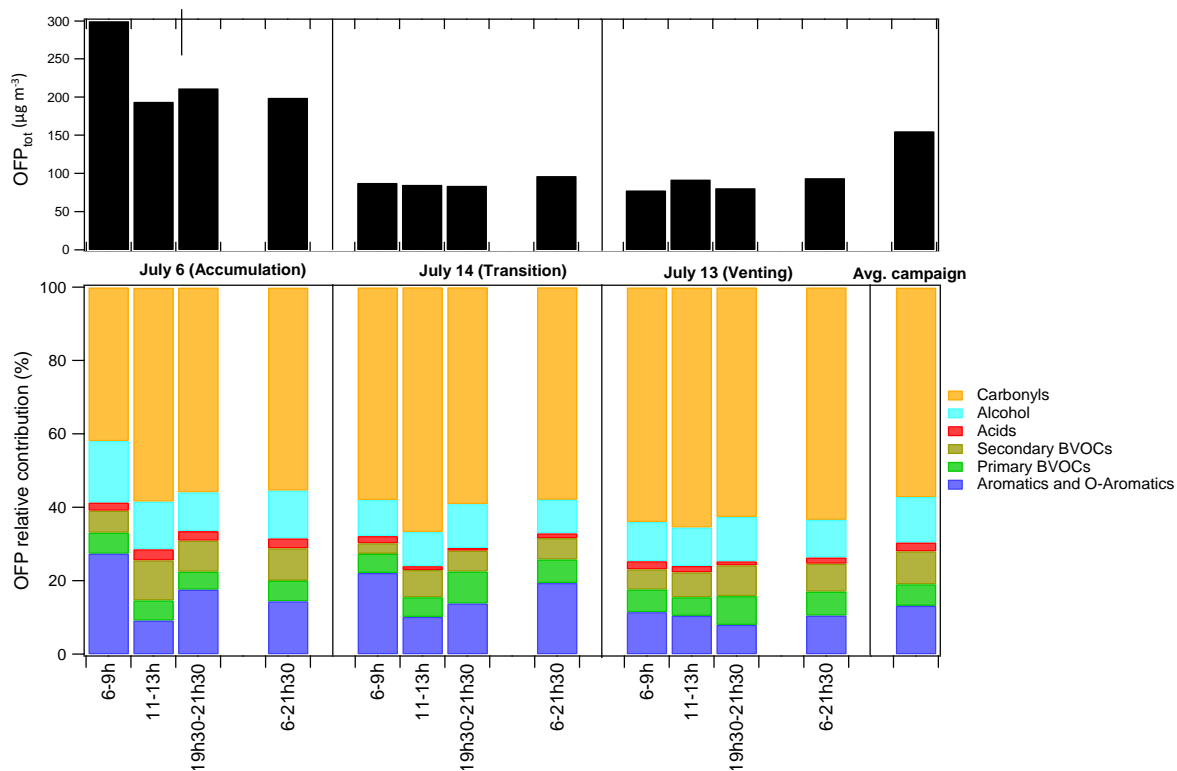


Figure S1. Ozone Formation Potential (OFP) and relative contribution of VOCs as measured by the PTR-ToF-MS (ISCIH site) to the total OFP for 3 selected days : 06/07/2016 (accumulation day), 14/07/2016 (transition day) and 13/07/2016 (venting day). For each day, we considered 3 distinct periods: Morning traffic peak (6:00-9:00 UTC), maximum insolation/biogenic VOC emissions period (11:00- 13:00 UTC), and evening traffic peak (19:30-21:30 UTC). Average daytime OFP (6:00-21:30 UTC) for each selected day as well as overall campaign average are also reported. PTR-MS measurements do not allow obtaining alkane/alkene concentrations and accordingly these are excluded in our OFP calculations.

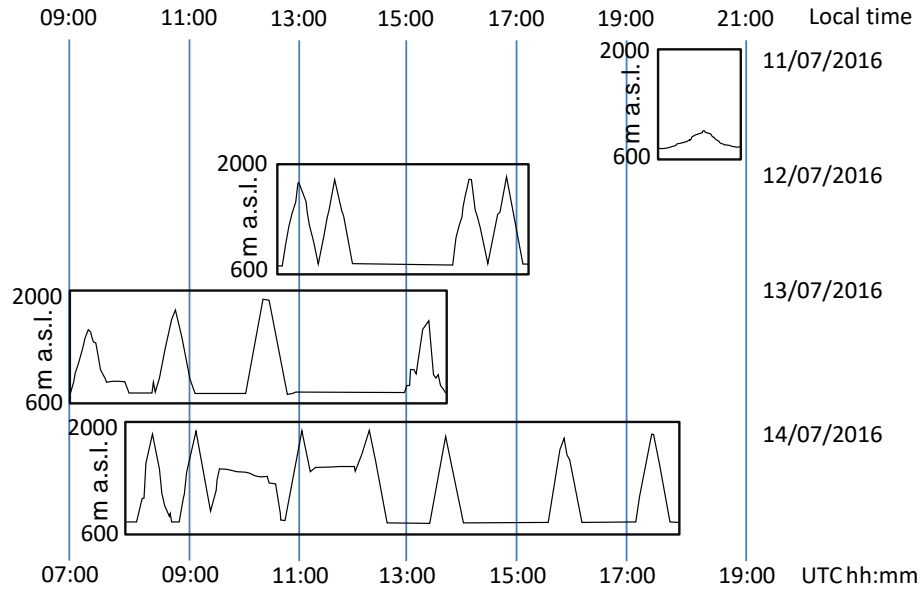


Figure S2. Timing of the vertical measurement profiles obtained during 11-14/07/2016 at Majadahonda (MJDH-RC).

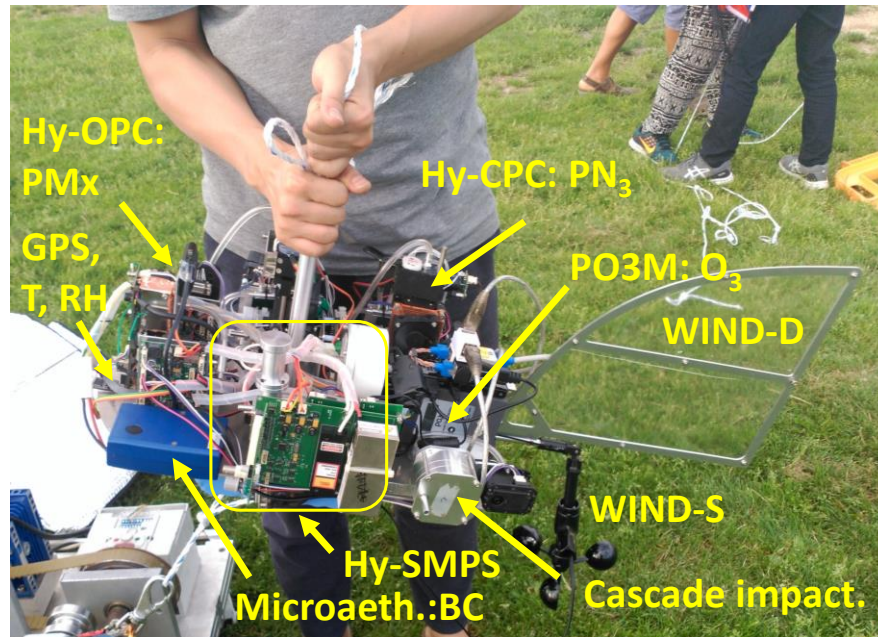


Figure S3. View of the instrumental set used for the balloon flights.

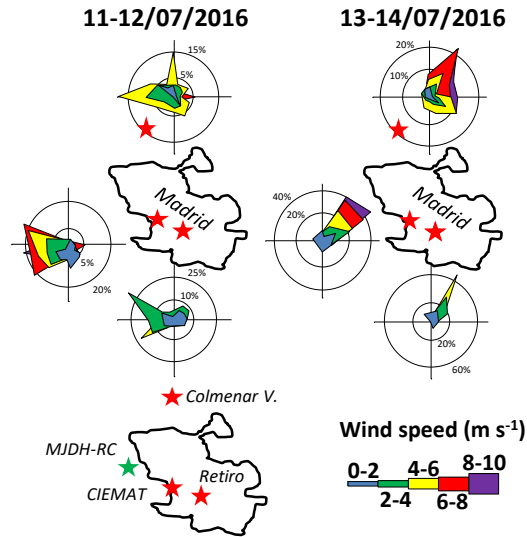


Figure S4. Wind roses for Madrid-CIEMAT and AEMET (El Retiro and Colmenar Viejo stations) and location of the vertical profiling site (MJDH-RC).

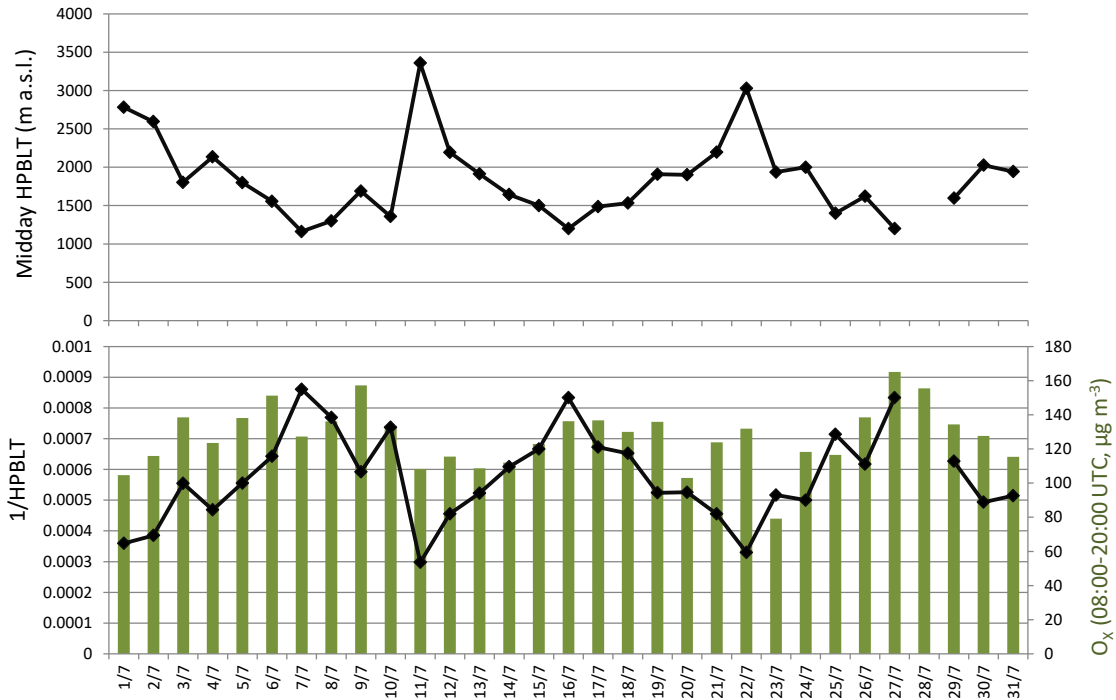


Figure S5. Top: Time series of the estimated midday height of the PBL top (HPBLT, m a.s.l.) obtained from the daily AEMET radio-soundings (using the simple parcel method) at Madrid airport for July 2016. Bottom: 1/HPBLT and average 08:00-20:00 UTC  $O_x$  concentrations at the MJDH air quality station.

### Description of results of the soundings of 11-13/07/2016

The first balloon flight on 13/07/2016 was performed at 10:45 UTC because earlier the wind speed was too high (Figure S7). At that time the top of the PBL had developed beyond the maximum height reached with the tethered balloons, so in the profile above 1100 m a.g.l. a very homogeneous concentration was detected. At this time on 14/07/2016 the upper bound of the PBL was perfectly identifiable in the UFP vertical profile over 700 m a.g.l., thus the growth of the PBL was faster on 13/07/2016 than on 14/07/2016. Similarly to 14/07/2016, the 13/07/2016 O<sub>3</sub> profiles were characterised by a progressive increase of concentrations with height (more accentuated in different strata). The profiles started with concentrations close to 40 ppb O<sub>3</sub> at the surface, and reached 83 ppb at the upper heights. As occurred on 14/07/2016, through the course of the day surface concentrations increased differentially with respect to the upper layers, to almost homogenize concentrations in the whole profile (between 68 and 80 ppb at all heights at 15:00 UTC).

In Figure S8 it can be observed that similar results to those described for UFP profiles on the 14/07/2016 were found on 12/07/2016 (upwards growth of the top of the PBL from the early morning):

- Around 700 m a.g.l. at 07:30 UTC (5000 #/cm<sup>3</sup> surface concentrations, 2000 #/cm<sup>3</sup> at the top of the PBL, and 900 #/cm<sup>3</sup> in the free troposphere).
- Around 900 m a.g.l. at 09:00 UTC (9000, 5000 and 2000 #/cm<sup>3</sup> for the above three levels).
- Above 1200 m a.g.l. (this being the maximum measurement height) at 10:00 UTC (10000 #/cm<sup>3</sup> surface concentrations and 7000 #/cm<sup>3</sup> at 1200 m a.g.l.) and 12:55 y 13:42 h (10000 #/ cm<sup>3</sup> surface concentrations and 20000 #/cm<sup>3</sup> at the maximum height of 900 m a.g.l.).

In the early morning of 12/07/2016 O<sub>3</sub> strata at different heights within the PBL were detected, with concentrations reaching 30 to 55 ppb and higher levels (55 to 65 ppb) at the highest altitude reached. During the 10:00 UTC flight O<sub>3</sub> levels reached 75 ppb at the top level decreasing gradually down to 40 ppb at surface levels. At 12:00 UTC concentrations at the top of the profile reached 87 ppb, 70-75 ppb in the 100-700 m a.g.l. transect and 60 ppb in the lowest 100 m a.g.l., where NO titration and O<sub>3</sub> deposition was more efficient.

As described for the soundings from 13 and 14/07/2016, the ones from 12/07/2016 again showed a vertical trend characterised by i) higher O<sub>3</sub> concentrations at the highest sounding altitude in the early morning, ii) increase in O<sub>3</sub> concentrations as the morning progressed (more pronounced at low altitudes), and iii) homogenous O<sub>3</sub> concentration along the entire vertical profile, except in the surface layers, where the deposition and titration markedly decreased O<sub>3</sub> levels reached at midday.

These vertical trends, with concentrations exceeding 75 ppb O<sub>3</sub> above 100-250 m a.g.l., and a marked decrease down to 60 ppb at surface levels was also evident during the short profiles obtained on 11/07/2016 at 18:28-18:41 UTC (Figure S8).

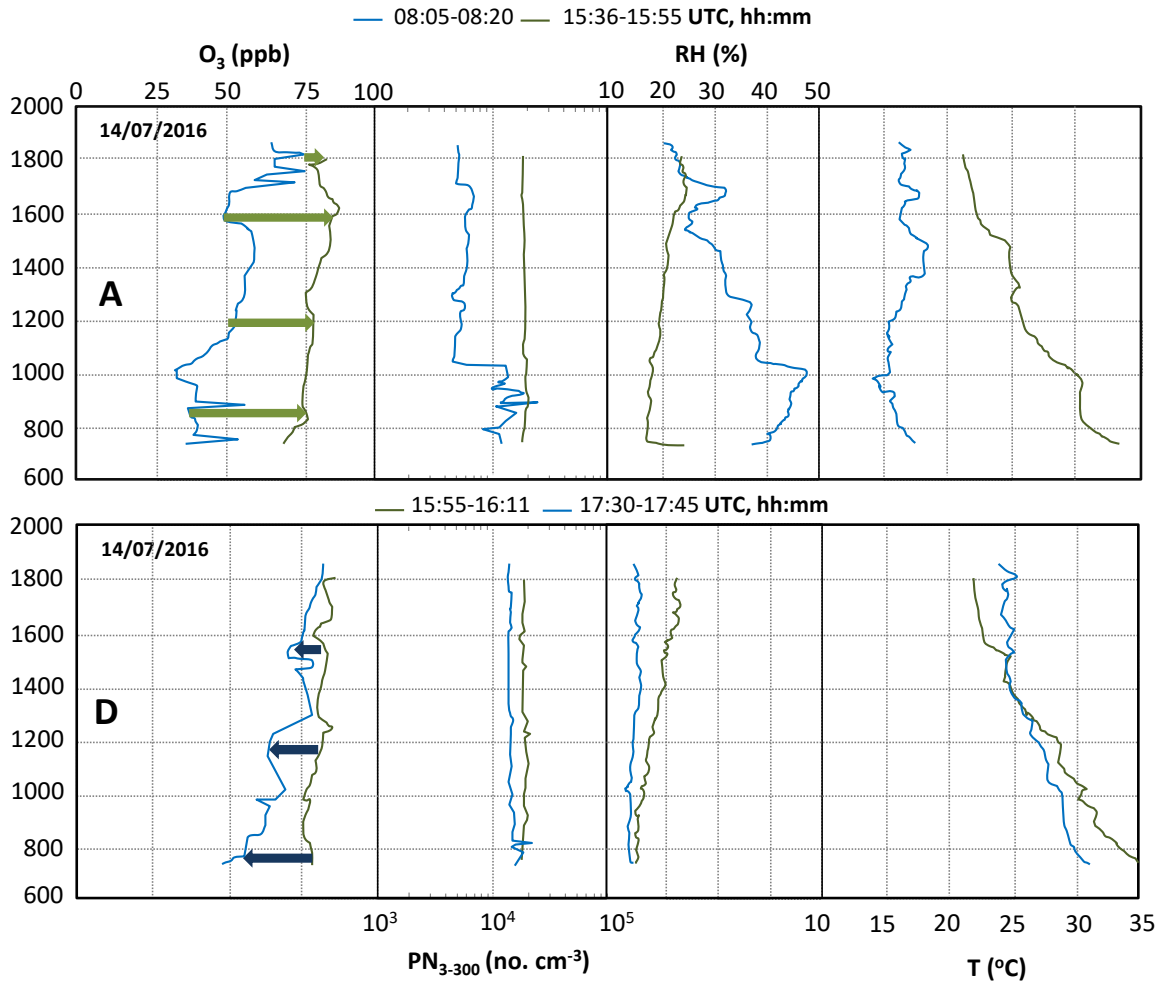


Figure S6. Vertical profiles of levels of O<sub>3</sub>, UFP (PN<sub>3</sub>), temperature and relative humidity obtained on 14/07/2016 (8:05 to 17:45 UTC), showing a top-down growth of differential O<sub>3</sub> concentrations from 08:05 with respect those from 15:55 UTC, as well as a bottom up decrease of this differential concentration between 15:55 and 17:45 UTC. A: Ascending; D: Descending.

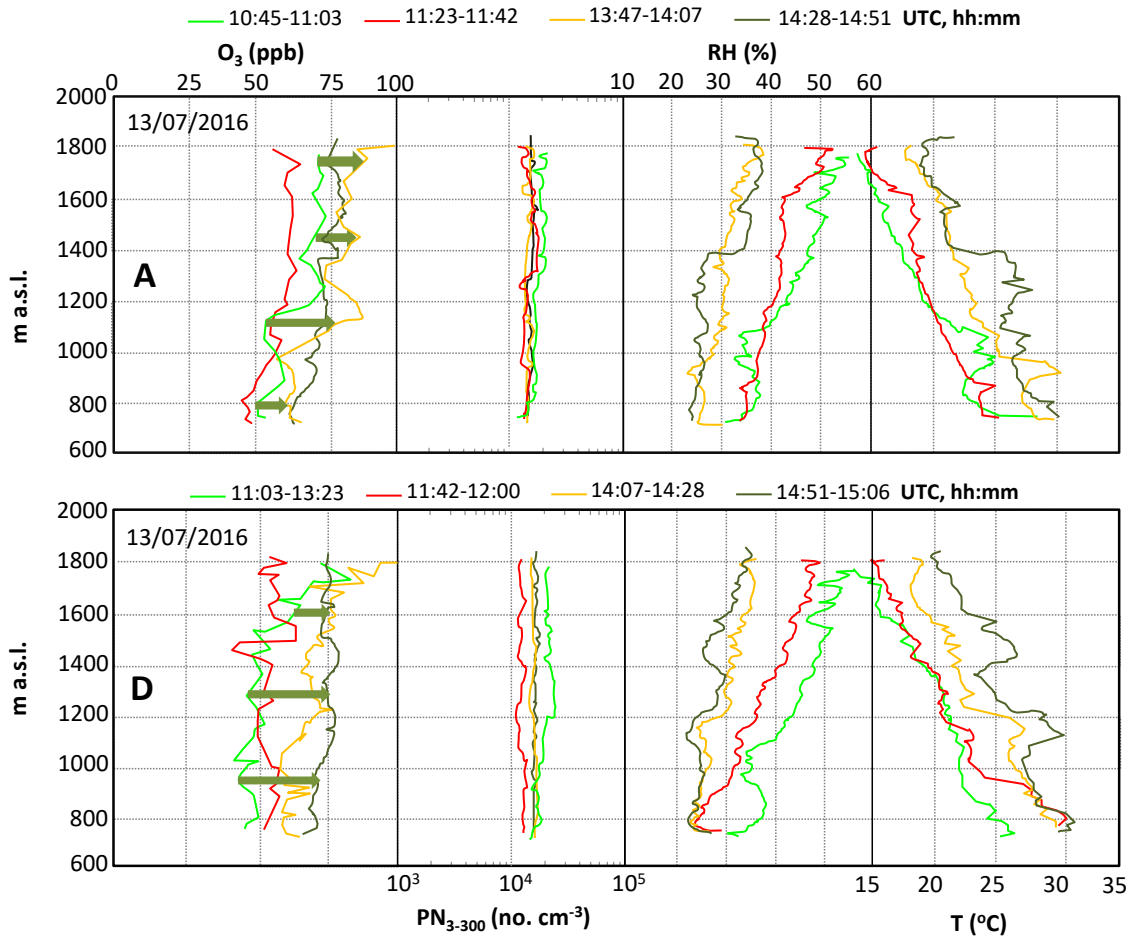


Figure S7. Vertical profiles of levels of  $O_3$ , UFP ( $PN_3$ ), temperature and relative humidity obtained on 13/07/2016 between 10:45 and 15:06 UTC. A: Ascending; D: Descending.

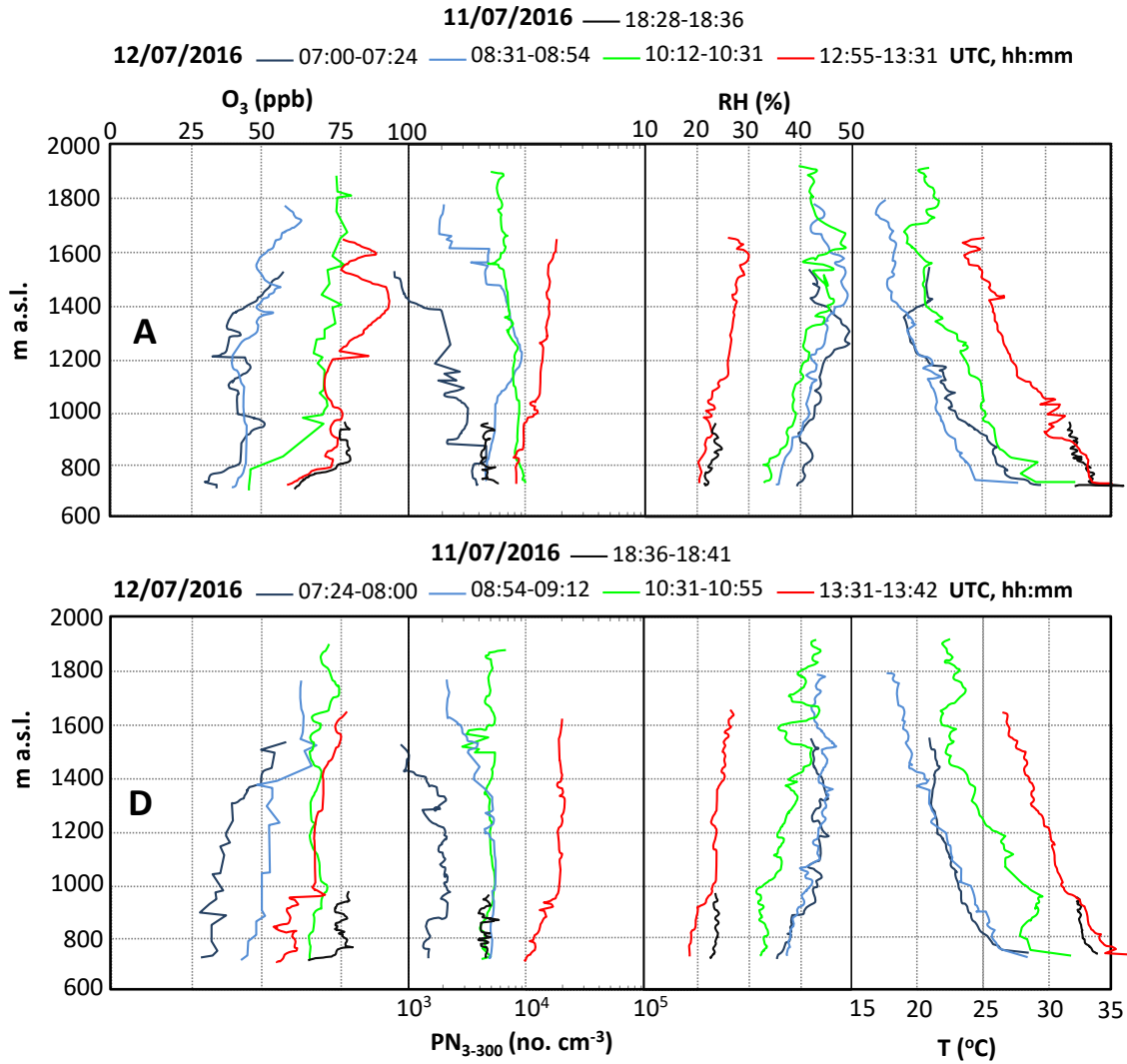


Figure S8. Vertical profiles of levels of O<sub>3</sub>, UFP (PN<sub>3</sub>), temperature and relative humidity obtained on 12 and 11/07/2016. A: Ascending; D: Descending.

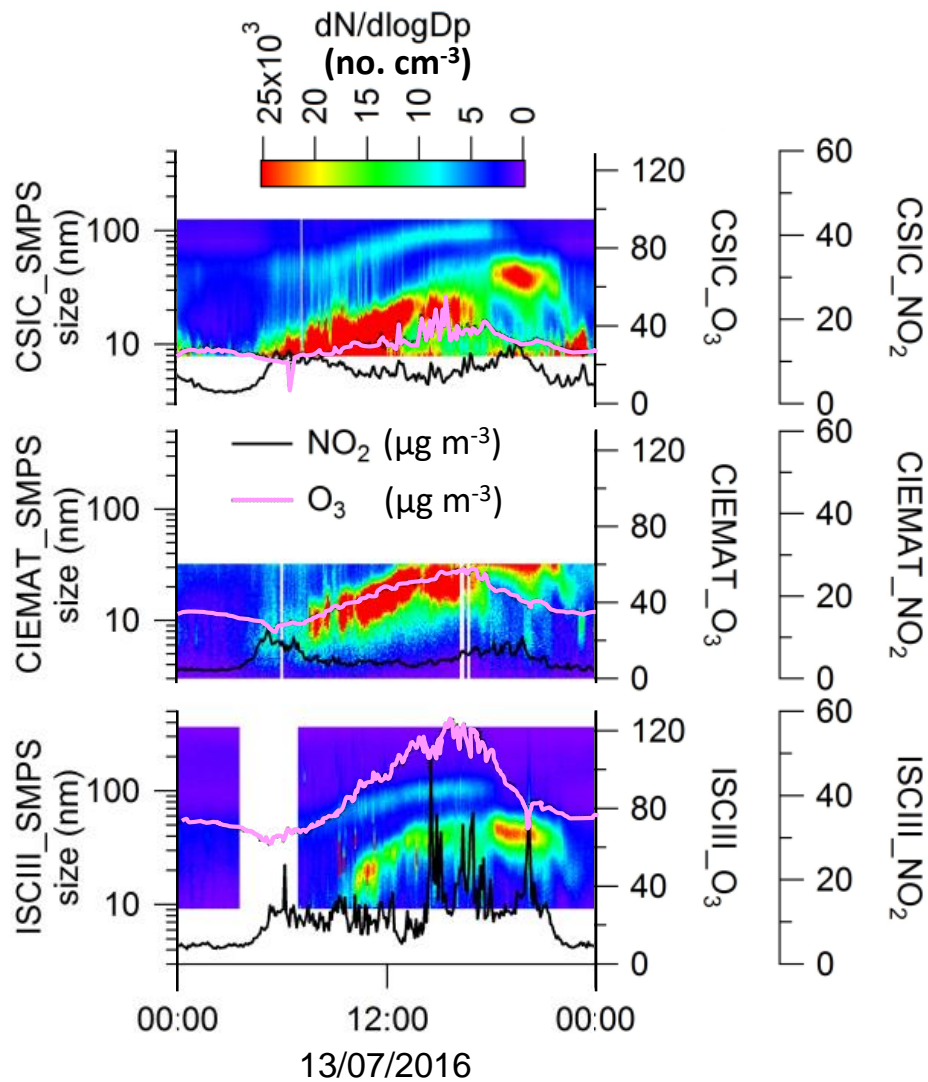


Figure S9. Example of the quasi-simultaneous occurrence of particle nucleation and growth episodes at the three supersites, with the nucleation stage coinciding with the starting of the increase of O<sub>3</sub> concentrations, and the growth stage with the increasing and maxima O<sub>3</sub> concentrations.

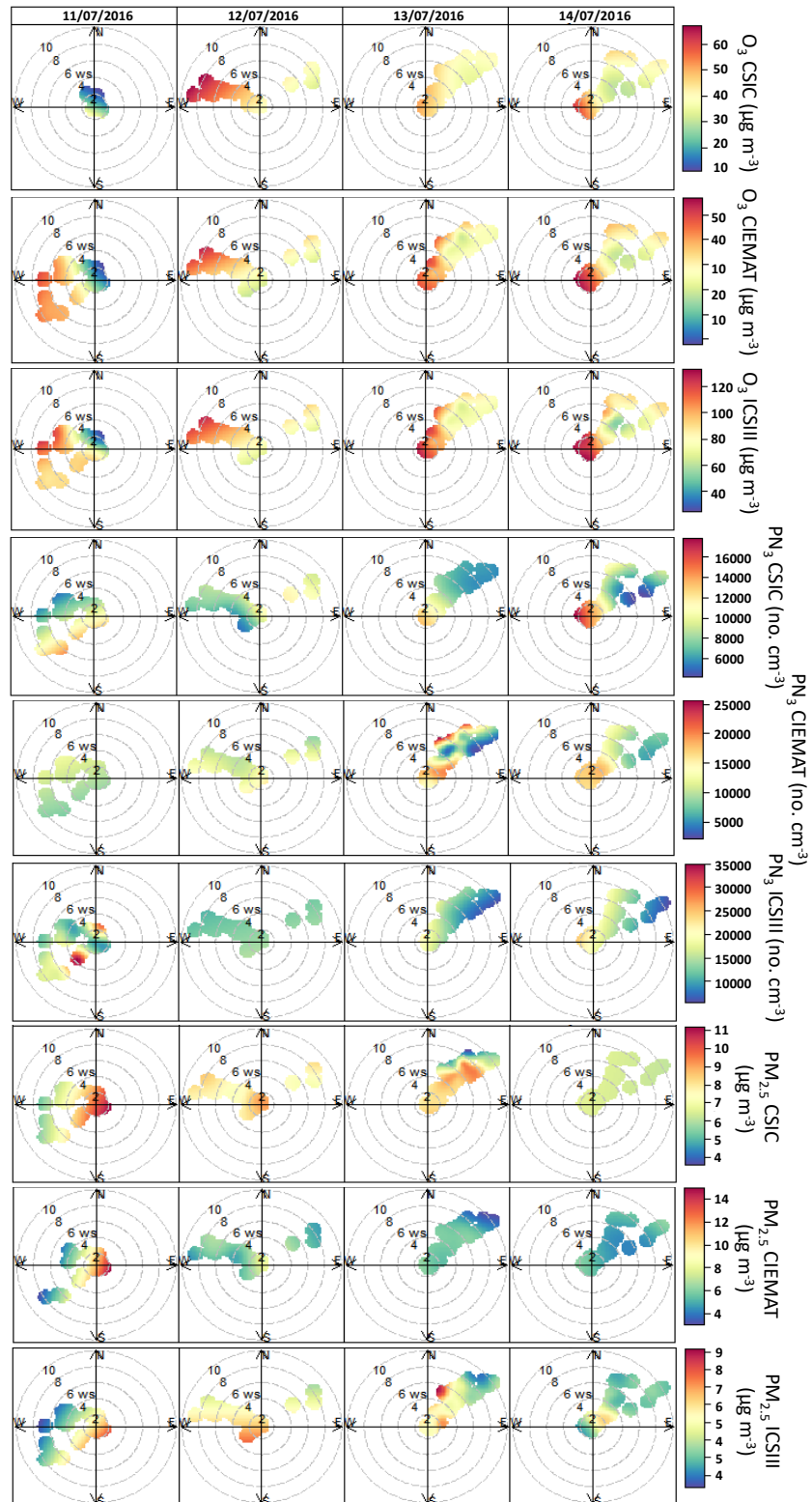


Figure S10. Polar plots of the concentrations of hourly  $O_3$  (upper), UFP ( $PN_3$ , medium) and  $PM_{2.5}$  (lower) concentrations measured at Madrid-CSIC, Madrid-CIEMAT and MJDH-ICSIII from 11 to 14/07/2016. Wind data used in all cases is the one from the CIEMAT meteorological tower.

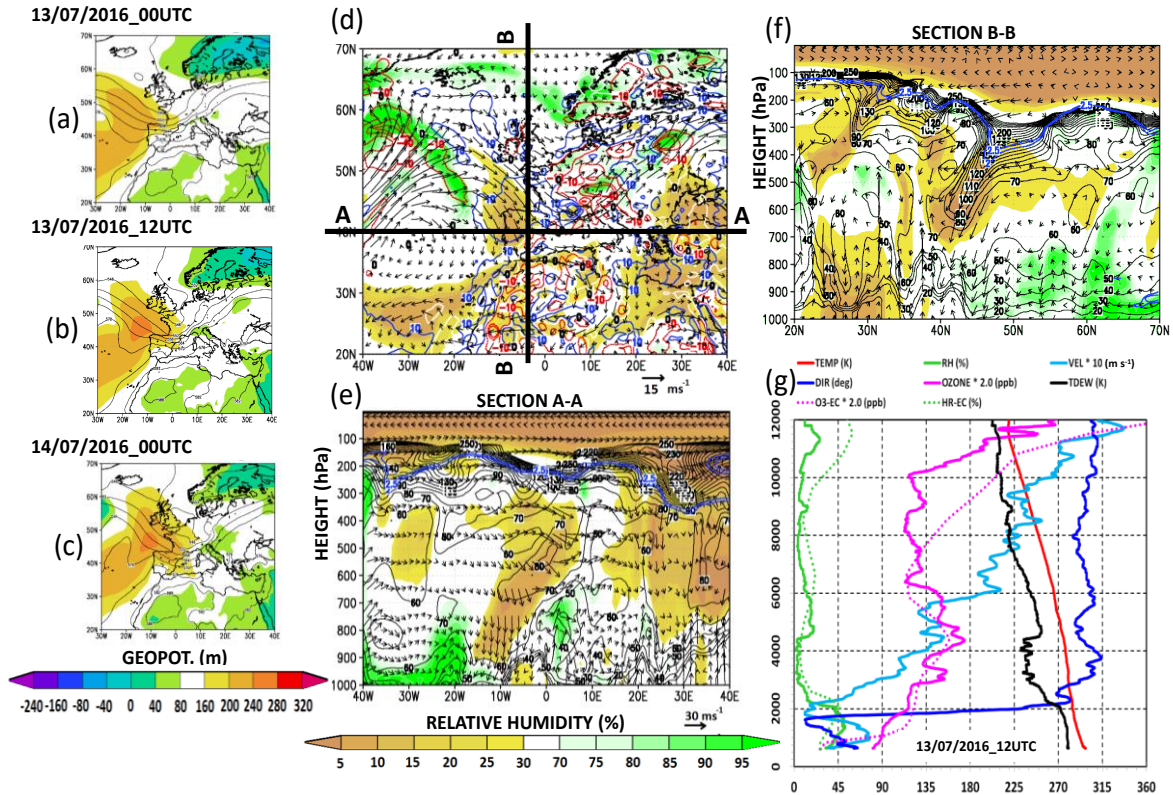


Figure S11. (a-to-f) ECMWF ERA-Interim reanalysis fields and (g) the AEMET  $\text{O}_3$ -free soundings at Madrid airport for the 13/07/2016: (a-to-c) sequence of the 1000 hPa Geopotential surface topography (m) in shaded colors and the 500–1000 hPa thickness (dam) in contour lines, showing the upper level trough and ridging over the Bay of Biscay; (d) average winds and relative humidity (shaded) at the middle troposphere (800–600 hPa) together with average pressure vertical velocities ( $1 \text{ unit} = -1 \times 10^{-2} \text{ Pa s}^{-1}$ ) in contour lines for the same depth of the troposphere (blue and red color for descending and ascending air motions, respectively) at 12 UTC on 13/07/2016, concurrent with the AEMET  $\text{O}_3$ -free sounding; (e) vertical cross section A-A at constant latitude 40.5N in panel (d), showing relative humidity (%) in shaded colors, ozone (ppbv) in contour lines, and winds, represented with the zonal (u) component and the pressure vertical velocities ( $1 \text{ ms}^{-1} = -1 \times 10^{-2} \text{ Pa s}^{-1}$ ). The dynamical tropopause is marked in blue lines with potential vorticity values of 2–2.5 PVU, and no ozone contours greater than 250 ppbv are represented (in the stratosphere); (f) vertical cross section B-B at constant longitude 3W in panel (d), following the same scheme for colors and contours shown in the A-A cross section. At this panel, winds are represented with the meridional component (v) and the pressure vertical velocities ( $1 \text{ ms}^{-1} = -1 \times 10^{-2} \text{ Pa s}^{-1}$ ); (g) the AEMET  $\text{O}_3$ -free soundings at Madrid airport for the 13/07/2016 (solid lines) and the ozone and relative humidity profiles (dotted lines) of the simultaneous ERA-Interim reanalysis.

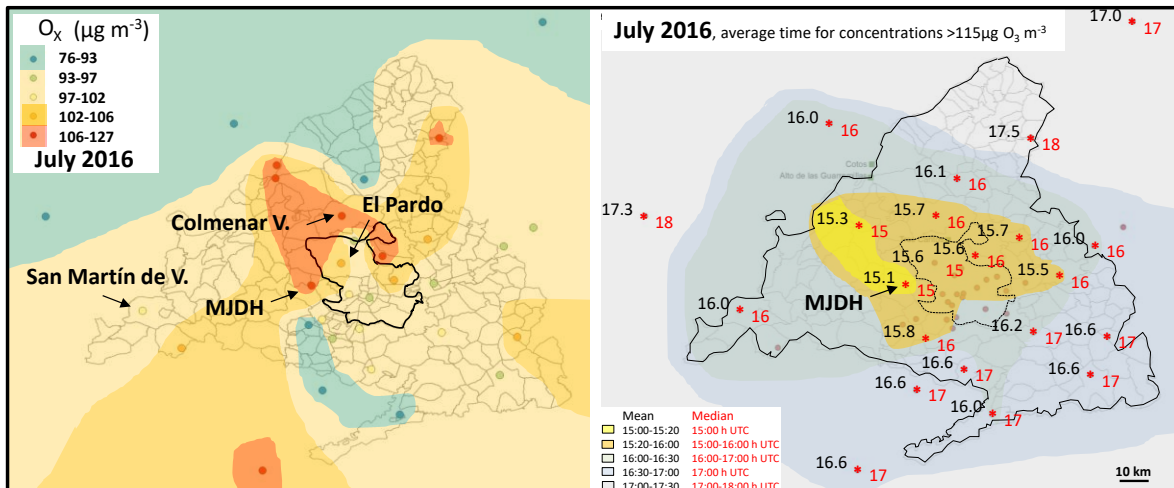


Figure S12. Left: Mean Ox (O<sub>3</sub>+NO<sub>2</sub>) July 2016 concentrations recorded at the monitoring sites from the Madrid air quality networks with an average concentration of NO<sub>2</sub> <25µg/m<sup>3</sup>. Right, average time where maxima hourly concentrations >115µg/m<sup>3</sup> are recorded for the same period and monitoring sites. MJDH: Location of Majadahonda.